LLNL-JRNL-812905

LAWRENCE
LIVERMORE
NATIONAL
LABORATORY

THERMODYNAMICS OF PLUTONIUM MONOCARBIDE FROM ANHARMONIC AND RELATIVISTIC THEORY

P. Soderlind, A. Landa, A. Perron, E. Moore, C. Wu

July 28, 2020

Applied Sciences

applied sciences

MDPI

Article

Thermodynamics of plutonium monocarbide from anharmonic and relativistic theory

Per Söderlind [1,*], Alexander Landa [2], Aurélien Perron [3], Emily E. Moore [4], Christine Wu [5]

[1]Lawrence Livermore National Laboratory, Livermore, California 94550, USA; soderlind@llnl.gov
[2]Lawrence Livermore National Laboratory, Livermore, California 94550, USA; landa1@llnl.gov
[3]Lawrence Livermore National Laboratory, Livermore, California 94550, USA; perron1@llnl.gov
[4]Lawrence Livermore National Laboratory, Livermore, California 94550, USA; moore255@llnl.gov
[5]Lawrence Livermore National Laboratory, Livermore, California 94550, USA; wu5@llnl.gov
* Correspondence: soderlind@llnl.gov

Received: date; Accepted: date; Published: date

Abstract: Thermodynamics of plutonium monocarbide is studied from first-principles theory that includes relativistic electronic structure and anharmonic lattice vibrations. Density-functional theory (DFT) is expanded to include orbital-orbital coupling in addition to the relativistic spin-orbit interaction for the electronic structure and it is coupled with anharmonic, temperature-dependent, lattice dynamics derived from self-consistent ab initio lattice dynamics (SCAILD) calculations. The so obtained thermodynamics is compared to results from simpler quasi-harmonic theory and experimental data. Formation enthalpy, specific heat, and Gibbs energy calculated from the anharmonic model are validated by a CALPHAD (CALculation of PHAse Diagram) assessment of PuC and sub-stochiometric $PuC_{0.896}$. Overall, the theory reproduces CALPHAD and measured data for PuC rather well but the comparison is hampered by the sub-stoichiometric nature of plutonium monocarbide. It is shown that a bare approach that ignores spin-orbit and orbital-orbital coupling (orbital polarization) of the plutonium 5f electrons promotes too soft phonons and free energies that are incompatible with that of the CALPHAD assessment of the experimental data. The investigation of PuC suggests that the electronic structure is well described by plutonium 5f electrons as "band like" and delocalized, but correlate through spin polarization, orbital polarization, and spin-orbit interaction, in analogy to our previous findings for plutonium metal.

Keywords: PuC; DFT; CALPHAD; Electron correlation, Anharmonic phonons, Thermodynamics, Nuclear fuel

1. Introduction

The physics of the actinides and their compounds is fascinating but also somewhat controversial. The controversy is primarily focused on the nature of the actinide 5f electrons and the degree of the electron correlation. Strong electron correlation manifests itself as localization of the 5f electrons on the actinide atom and for the actinide-oxide compound this localization leads to band gaps in the electronic structure [1,2]. On the other hand, one finds weaker electron correlation for the early elemental actinide metals, thorium through plutonium. Particularly for the first four, there is now consensus that they are well described by band-like 5f electrons [3,4]. In terms of theoretical approaches, weak or intermediate electron correlation implies that density-functional theory is an appropriate starting point and methods aimed for stronger electron correlations, assuming explicitly an intra-atomic Coulomb interaction with a Hubbard U parameter (DFT + U), is not necessary. When it comes to plutonium metal the electronic structure is still debated in the literature. There are viewpoints that the 5f electrons are not strongly correlated and that no Hubbard U ($U = 0$) [5,6], or a small value (U ~ 1 eV) [7], is appropriate. But there are also those who believe that the 5f electrons are strongly correlated, essentially localized, and suitably described by a very large U parameter (U ~ 4-4.5 eV) [8,9]. Some of these models are very convoluted and require assumptions of parameters such as the debated U. One cannot ignore, however, that a more transparent and less complicated model (U = 0) describes plutonium very well [5] including its magnetic profile [10].

Regarding the actinide mononitrides and monocarbides, they appear to lie between the oxides and the elemental metals in terms of the 5f-electron correlation [11]. In the nitrides and carbides, one does not encounter band gaps as is the case for the oxides and they are also not insulators but metallic. In analogy with the actinide oxides they are magnetic but the detailed magnetic structures are not known for all of them. They form in the rock-salt (B1 or NaCl) structure that is simple cubic with two types of atoms in the (000) and (½ ½ ½) positions, respectively. Their simple crystal structure and the fact that the 5f electrons are less correlated than in their oxide counterparts make them well suited for DFT-type studies. One complication for modeling, however, is that they tend to be nitride and carbide deficient, resulting from vacancies and imperfections of the material. Consequently, they form as AnN_{1-x} or AnC_{1-x} (An is actinide) compounds, where x is small (~ 0.1) but significant. The electronic structure for several AnC compounds were recently studied with quantum-chemical calculations by Pogány et al. [12].

In addition to the fundamental-science interest in the actinide mononitrides and monocarbides they are compelling from a practical and applications perspective. The technological interest arises from their potential use as advanced nuclear fuels for fast-breeder reactors. These materials have good mechanical characteristics but also possess superior thermophysical properties [13] such a high melting temperatures, high density of heavy atoms, and high thermal conductivity. In spite of the interest, there is not as much experimental data available for them as there are for the actinide oxides and robust theoretical modeling, particularly at elevated temperatures, is certainly welcomed. In the present report we focus specifically on the thermodynamical high-temperature properties of plutonium monocarbide, PuC, from first-principles theory.

Recently, we undertook an analogous study on uranium mononitride [14] and here the thermodynamic modeling was founded on density-functional-theory electronic structure coupled with lattice dynamics that allowed for anharmonic lattice vibrations. For UN, we compared and validated our first-principles model directly with experiments in addition to results from a CALPHAD assessment of the available measured data. Here, we adopt the same modeling approach for plutonium monocarbide but we recognize that the plutonium 5f electrons provide a greater challenge for the theory. Therefore, we go beyond our previous treatment of the electronic structure in UN and now include relativistic effects and an extension to DFT that addresses orbital-orbital moment coupling (orbital polarization) that is known to be important for accurately describing plutonium metal [5]. It turns out that these additional electron correlations for PuC are necessary for realistic Gibbs energies. For comparison, and to confirm our first-principles model for PuC, we carry out CALPHAD calculations of the Gibbs energies, heat capacities, and formation enthalpy, utilizing a thermodynamic database and the Thermo-Calc software.

In the following sections, 2-4, we detail our density-functional-theory implementations and CALPHAD method and continue by showing our results and provide context in a summary and discussion section.

2. Computational methods

2.1. Electronic structure methods

We are applying three methods, each with their own advantages, for calculating the electronic structure of PuC. Two all-electron approaches that in one case is implemented with a so-call "full potential", i.e., where no geometrical-structural approximations exist, and the other with a Green's function technique that allows for a realistic alloy and disorder treatment. The third is a plane-wave pseudopotential method that is fast and efficient for calculating forces on cells with many atoms. All three methods rely on density-functional theory and the generalized gradient approximation (GGA) [15] for the electron exchange and correlation energy functional.

One method is the all-electron full-potential linear muffin-tin orbital (FPLMTO) method and this implementation has been explained in the literature [16]. It adopts no approximations for the core states that exist at deeper energy levels than the valence states. This is a more accurate treatment than that of the plane-wave methods where the core electrons are a replaced by a pseudopotential.

Some quantities are expanded in series (basis functions, electron densities, and potentials) of spherical harmonics inside non-overlapping spheres centered at each atomic position. The radial part of the basis functions inside these spheres are calculated from a wave equation that includes all relativistic corrections including spin-orbit coupling for d and f states but not for the p states, as is appropriate [6]. The orbital-orbital coupling (orbital polarization) is only operating on the f states [6,17] and is not explicit in conventional density-functional theory but has been shown to be important for some f-electron systems, particularly plutonium [5]. Generally, the set-up parameters of the present calculations for PuC are close to those for plutonium metal [5]. The FPLMTO method is applied for calculating the PuC formation enthalpy, the elastic constants, and the so-called "cold curve", i.e., the total-energy variation with atomic volume, that is the fundamental input to the Debye-Grüneisen quasi-harmonic simulations. The elastic constants are calculated applying conventional strains for cubic crystals while the shear modulus is the Voigt-Hill-Reuss average [18] of the single-crystal moduli. Also, the presented electronic density of states and the related simulated photoelectron spectra are obtained from this method. Lastly, the Racah 5f parameters within the orbital-polarization formalism [17] are self-consistently calculated with FPLMTO for use as a fixed (majority spin band) parameter in our plane-wave calculations.

For the computationally more demanding supercell calculations or the self-consistent-phonon method (SCAILD, self-consistent ab inito lattice dynamics) [19], we utilize an efficient electronic-structure approach. Namely, the pseudopotential plane-wave Vienna ab initio simulation package (VASP) with the projector-augmented-wave method with plane-wave basis set as implemented in VASP [20-22]. The computational set-up is defined by an energy cut-off of 400 eV and an energy convergence of 100 eV. The VASP calculations furthermore include non-collinear magnetism with spin-orbit coupling and orbital polarization as implemented recently by us [6].

PuC is sub-stoichiometric, as mentioned, and the sensitivity to the deviation of the Pu/C ratio from unity has been explored by VASP but also utilizing a technique that incorporates accurate alloy theory within the coherent-potential approximation (CPA) [23]. The exact muffin-tin orbital (EMTO) method relies on Green's function formalism where the one-electron potential is represented by optimized overlapping muffin-tin potential spheres [24]. The EMTO-CPA [25] is thus well suited to explore computational disorder and sub-stoichiometric conditions. It can also be used to study the influence of randomly distributed vacancies on a sub-lattice (see the Summary and discussion section below). Other relevant details of the EMTO calculations are similar to those we have reviewed for other plutonium-alloy systems [5]. Presently, we restrict ourselves to EMTO calculations without spin-orbit coupling. As with the VASP method, EMTO is compared to FPLMTO for perfect sub-stoichiometric PuC to validate the robustness and accuracy of the method.

2.2. Lattice dynamics methods

Our main tool for lattice dynamics is the self-consistent ab initio lattice dynamics (SCAILD) methodology [19] that we often refer to as the self-consistent phonon method. The idea of the scheme is to employ the small-displacement method to calculate the phonons in a first step and then apply thermally induced (fixed finite temperature) "frozen" phonons on the atoms and calculate corresponding DFT atomic forces. The next step is to recalculate new phonons utilizing these DFT forces and repeat until convergence [19]. This self-consistent-phonon approach is appealing because it couples different displacements of all atoms with each other (unlike the frozen-phonon method) and therefore it can account for strong phonon-phonon coupling and anharmonic behavior. We have used SCAILD successfully for both uranium mononitride as well as for the cubic phases of uranium and plutonium metals in the past [5,13,26,27] with good success. For SCAILD one needs to specify a supercell of the crystal structure and for PuC we define a 3 x 3 x 3 supercell for a total of 54 atoms. The DFT forces are gathered from VASP calculations and the SCAILD iterative scheme requires a little more than 200 iterations to strictly converge the lattice-vibration contribution to the free energy (meV). We perform several simulations: For each temperature (T = 600, 800, 1000, 1200, 1500, and 2000 K), we chose three to five (depending on temperature) lattice constants in order to determine the equilibrium volume on the basis of the Gibbs-energy minimum. To assess the importance of 5f-electron correlations beyond conventional DFT-GGA, we employ methods that either include spin-orbit coupling and orbital polarization (DFT+SO+OP) or not (DFT).

In Figure 1 we show results from SCAILD for PuC at a temperature of 800 K, for the two levels of electronic-structure theory. The lattice constants are held fixed, corresponding to their zero-temperature equilibrium volumes (16.2 and 15.6 Å^3).

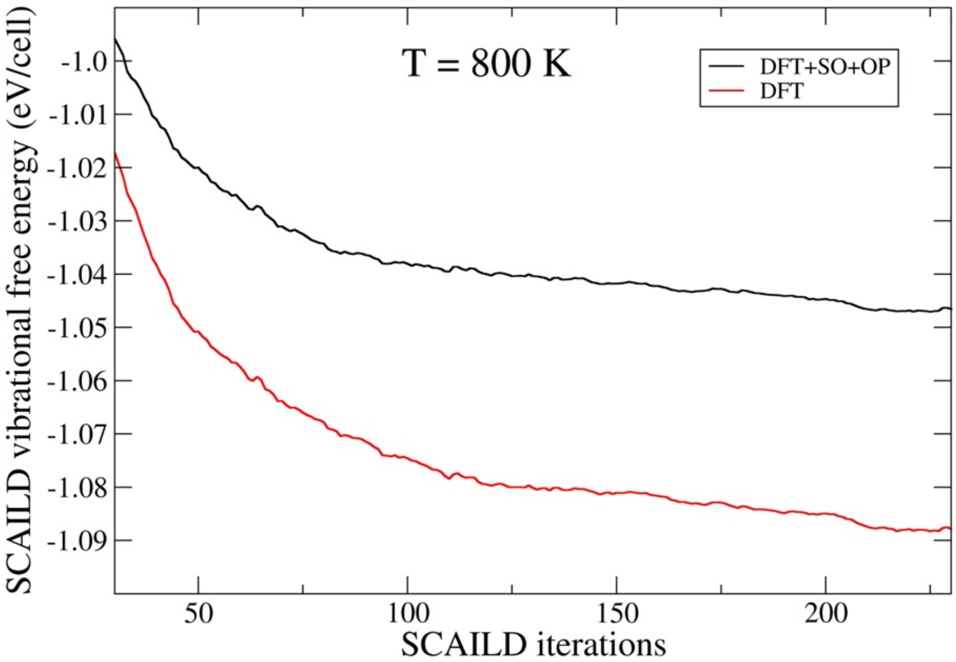

Figure 1. SCAILD vibrational free energies (eV/cell) as functions of iterations for VASP force calculations that include spin-orbit coupling and orbital polarization (DFT+SO+OP) and not (DFT). The atomic volumes are kept constant and equal to 16.2 Å^3 and 15.6 Å^3, respectively (see main text).

One can judge the importance of anharmonic phonons by comparing calculated thermal properties from anharmonic and quasi-harmonic theory. For this reason, we conduct a limited set of calculations from two implementations of the Debye-Grüneisen quasi-harmonic approach [28]. It is a very efficient scheme that only requires the cold curve as input in addition to the atomic mass of the atoms in the material. There are, however, some assumptions within this model that must be made. First, Moruzzi et al. [28] suggest that the Debye temperature can be derived from this simple relationship:

$$\theta_D = Const\sqrt{\frac{rB}{M}} \tag{1}$$

where r is the atomic Wigner-Seitz radius in atomic units, B is the bulk modulus in kbar, and M the atomic mass (u). They studied non-magnetic transition metals and argued that an appropriate value for *Const* is 41.63, but the best value for this constant is generally unknown. Second, there are two philosophies regarding the formulation of the Grüneisen parameter. One that is supposedly [28] better at higher temperatures, γ_{HT}, and one that is more suitable when comparing to experimental specific-heat data at lower temperatures, γ_{LT}. They are referred to as Slater (γ_{HT}) and Dugdale-MacDonald (γ_{LT}) [29,30], respectively, and are defined as:

$$\gamma_{HT} = \gamma_{LT} + \frac{1}{3} = -\frac{2}{3} - \frac{V}{2}\frac{\partial^2 P/\partial V^2}{\partial P/\partial V} \quad (2)$$

Here, *P* is the pressure and *V* the atomic volume. Third, the necessary analytical representation of the DFT-calculated cold curve is an approximation in itself. Moruzzi et al. [28] applied a Morse function [31] for this purpose but other forms can be considered and the actual choice will influence the results of the Debye-Grüneisen model to an extent. In our quasi-harmonic calculations of the specific heat we utilize the Gibbs2 package [32] and our own implementation [33]. For Gibbs2, referenced below as "quasi-harmonic (a)", we use *Const* = 58.03, γ_{LT}, and a third-order Birch-Murnaghan analytical form [34]. The alternative treatment [33] is referred to as "quasi-harmonic (b)". In this case the scaling factor, *Const* = 57.23, is determined from the calculated Poisson's ratio (ν = 0.256, see table below). The latter implementation [33] assumes γ_{HT} and a Morse function representing the DFT total energies.

2.3. CALPHAD method

We apply the thermodynamic CALPHAD technique to compute the heat of formation, heat capacity, and Gibbs energy of PuC as functions of temperature. The CALPHAD results are then compared to our first-principles thermodynamic data and in the case of the specific heat and formation enthalpy also experimental data. Importantly, CALPHAD is able to also interrogate the significance of the sub-stoichiometric formation of PuC_{1-x}. Generally, the fundamental objective for the CALPHAD scheme is to model the Gibbs energy of individual phases pertaining to binary and ternary systems to optimally reproduce carefully reviewed phase diagrams and thermodynamic properties. From the Gibbs energy one computes phase stability and thermodynamic properties of multicomponent systems [35-37]. CALPHAD self-consistently generates functions and parameters representing phase dependent Gibbs energies that are collected in a database that can be utilized for simulation of thermodynamical properties of multi-component systems.

The CALPHAD data is compared to the first-principles modeling, but additionally, we understand that the interaction between CALPHAD and theory improves the thermodynamic-modeling capability particularly for materials with many unknown variables. For example, *ab initio* results such as heats of formation can directly provide important constraints to the CALPHAD modeling framework in the absence of experimental data. Furthermore, we note that optimization of parameters and minimizing errors within in the CALPHAD technique is an inverse problem with infinite degrees of freedom [38]. As a consequence, many combinations of parameters chosen by the user can produce coinciding phase diagrams. The use of DFT-predicted properties related to the CALPHAD assessment constrains the optimization and certifies the resulting thermodynamical database, both in terms of phase stability and energetics. This has in recent years become customary and first-principles-informed CALPHAD assessments for actinide systems are available [39-41].

Specifically, for the plutonium-carbide system we apply the CALPHAD assessment [42] for ideal stoichiometry PuC as well as $PuC_{0.869}$ when comparing to the specific heat. In the case of the Gibbs energies we only consider PuC for an appropriate comparison with the first-principle results.

3. Results

3.1. Elecronic structure

As mentioned in the introduction, one of the central questions regarding the electronic structure of any actinide compound is the nature of the actinide 5f electrons. For the elemental metals, up to americium, the 5f electrons can be regarded as bonding and itinerant and not localized as they are in americium and the following actinides. For plutonium there is still a debate on this, but our view is that the 5f electrons are more delocalized than not and that opinion is supported by a wealth of evidence [5]. Specifically, for plutonium monocarbide, it has been argued that the 5f electrons are less correlated than both plutonium oxides as well as nitrides [11]. No theoretical method is currently able to predict the nature of the 5f electrons in these systems but comparisons with experimental data provide clues.

In Figure 2 we show the calculated, with spin-orbit coupling and orbital polarization, total electronic density of states (e-DOS) for PuC.

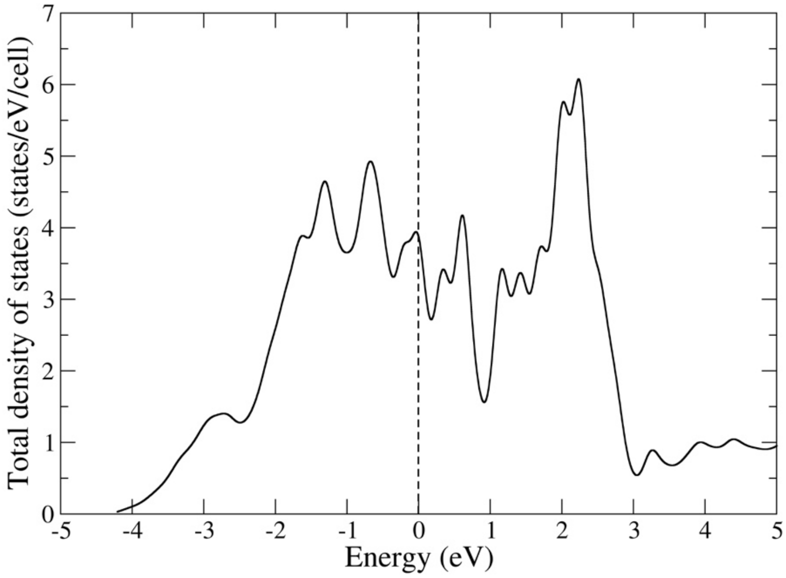

Figure 2. FPLMTO total electronic density of states for PuC. The vertical dashed line indicates the location of the Fermi level (at zero energy). The calculations include spin-orbit coupling and orbital polarization and the atomic volume is equal to 16.2 Å^3.

The PuC e-DOS is quantitatively similar to that of both the α and δ phases of plutonium [5] because it has significant occupation of 5f states at the Fermi level. This similarity suggests that the 5f electrons are delocalized as we believe they are in α and δ plutonium, but a comparison with experimental photoelectron spectra will help the interpretation. The photoelectron spectra for sub-stoichiometric $PuC_{0.85}$ has been measured by Gouder et al. [43] and in Figure 3 we compare that result with our e-DOS for PuC that has been broadened and convoluted to simulate instrumental resolution and photon lifetimes [44]. We also include, for comparison, the corresponding simulated photoemission for δ-plutonium [44].

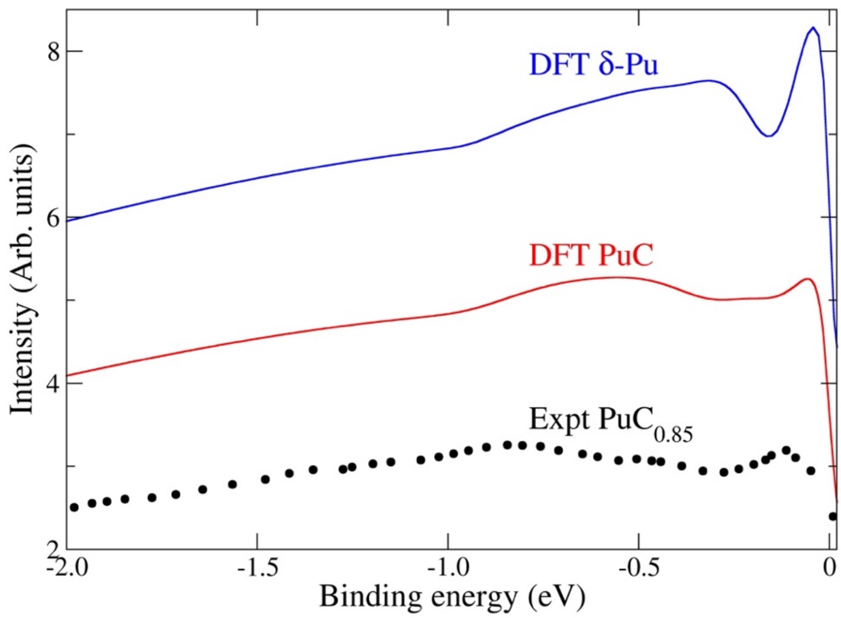

Figure 3. FPLMTO electronic density of states for PuC that has been convoluted due to instrumental resolution and photon lifetime broadening. The experimental data points for $PuC_{0.85}$ are from photoemission by Gouder et al. [43] and the simulation for δ-Pu from Ref. [44]. The curves are shifted relative to each other to make the plot more readable.

The experimental $PuC_{0.85}$ photoelectron result actually looks quite similar to our simulation for PuC. One would not necessarily expect a perfect agreement because the stoichiometries are different and the calculated spectral density do not include photoexcitation matrix elements. Nevertheless, the favorable comparison supports the interpretation that the 5f electrons, that dominate the spectra for the plutonium-carbide system, are indeed delocalized as treated by the theory. We further notice in Figure 3 that the result for δ-plutonium is quantitatively comparable to PuC, indicating that the 5f electrons behave similarly for these systems.

Plutonium monocarbide (PuC_{1-x}) is known to be anti-ferromagnetic (AF) at temperatures below 100 K [45] but to date, the size of the magnetic moments has not been determined. Previous DFT calculations within the local density approximation [46] reproduce the AF configuration for $PuC_{0.75}$ but for ideal PuC a ferromagnetic (FM) configuration was predicted with magnetic moments ~ 2 μ_B/atom. The present calculations for PuC, that are based on GGA and the aforementioned spin-orbit and orbital-polarization correlations, predict the FM state but it is only weakly stable over the AF configuration (~ 1 mRy/atom). Both configurations have total magnetic moments that are small (~ 0.1 μ_B) because of the effective compensation between the spin and anti-parallel orbital components (both close to 3.7 μ_B in absolute magnitude). The orbital-orbital coupling tends to enhance the orbital moment in metallic plutonium systems [5] and ignoring this interaction in the model produces a much smaller orbital moment (~ 2.7 μ_B). In addition to the magnetic moments, the bonding properties of the AF and FM configurations are nearly identical, meaning that the atomic volume and bulk modulus are essentially the same. Because the energetics and bonding between these two magnetic states are so similar and that the magnetic ordering only occurs below 100 K, we only consider the FM state as we proceed by focusing on thermodynamics at high temperatures.

3.2. Ground-state properties and thermodynamics

Next, we discuss our predicted ground-state properties, including the elastic constants, and our lattice-dynamics results. In Table 1 we show calculated equilibrium volumes and elastic constants for PuC from the full theoretical treatment (DFT+SO+OP) and for the simpler theory that excludes spin-orbit coupling and orbital polarization (DFT). Elastic moduli obtained from Born-Mayer and Coulomb model potentials have been reported for PuC [47], but their zero-temperature values are considerably smaller (C_{11} = 63.9, C_{12} = 27.2, C_{44} = 27.2 GPa) than ours presented in Table 1.

Method	V	B	B'	C_{11}	C_{12}	C_{44}	G	ν
DFT+SO+OP	16.2	125	2.7	218	78.0	75.0	73.0	0.256
DFT	15.6	141	0.65	177	123	141	73.9	0.277

Table 1. Ground-state properties obtained from the full theoretical treatment (DFT+SO+OP) and for a treatment that ignores spin-orbit coupling and orbital polarization. The atomic volume (V) is given in units of Å^3, while the bulk (B), shear (G) and elastic (C_{ij}) moduli are given in units of GPa. The shear modulus is a Voigt-Reuss-Hill average and the Poisson's ratio, ν, is obtained from B and G (see main text).

We expect that our theoretical elastic moduli in Table 1 are good because we know they are rather accurately calculated for the phases of elemental plutonium metal [48]. The Poisson's ratio, ν, in the table is obtained from the standard formula for cubic crystals:

$$\nu = \frac{3B-2G}{2(3B+G)} \tag{3}$$

Unfortunately, there are no published experimental data on the single-crystal elastic constants (C_{ij}) that could help distinguish between the present and previous [47] modeling. For the isothermal bulk modulus (B), however, an experimental value has been reported (118 GPa) [49] that is in better agreement with our best theory (125 GPa) than the model-potential result (39.4 GPa) [47].

In regards to our first-principle results in Table 1 we find some differences between the full theory (DFT+SO+OP) and the scalar-relativistic (no SO or OP) approach (DFT). The former produces a somewhat larger atomic volume and a correspondingly softer bulk modulus, while the shear modulus is about the same. Most notably is the fact that the tetragonal shear constant, $C' = (C_{11}\text{-}C_{12})/2$, is very small for the scalar-relativistic approximation (27 vs. 70 GPa). This very small C' indicates that the crystal is relatively close to a mechanical instability that is linked to softer phonons for the related phonon branches. Softer phonon modes imply more entropy and a greater contribution to the free energy, and that is exactly observed in our calculated free energies shown in Figure 1.

Moving on to thermodynamics and our lattice-dynamics results, we show in Figure 4 our calculated phonon density of states (p-DOS) at 1200 K. The p-DOS clearly suggests that including spin-orbit coupling and orbital polarization (DFT+SO+OP) in the electronic structure stiffens the lattice dynamics resulting in more weight of the phonon modes at higher energies.

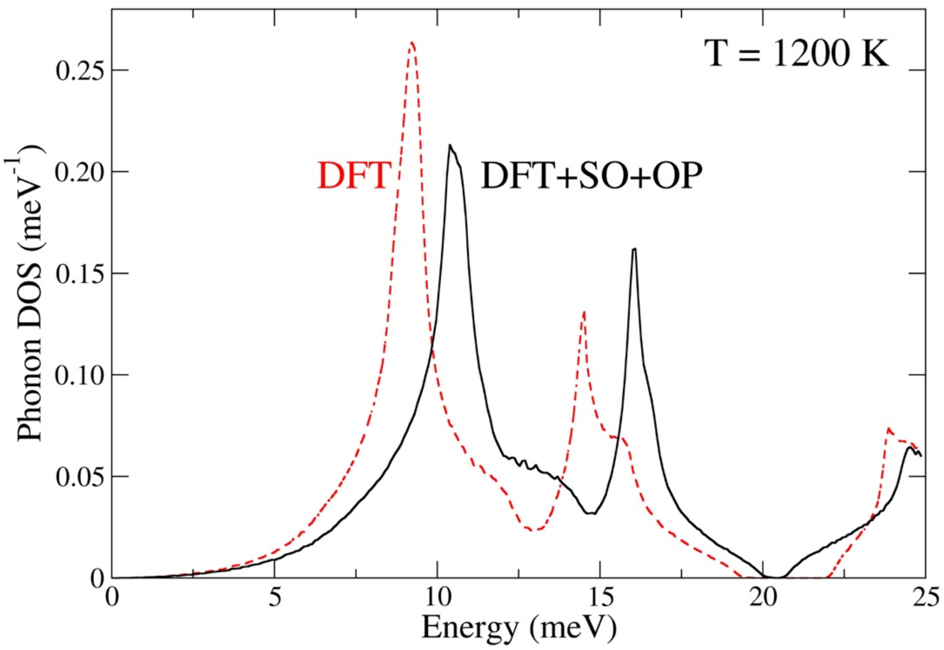

Figure 4. SCAILD phonon density of states (states/meV) at 1200 K from electronic structure that include spin-orbit coupling and orbital polarization (DFT+SO+OP) and not (DFT). The atomic volumes are 15.6 Å^3 (DFT) and 16.2 Å^3 (DFT+SO+OP), respectively.

The consequence of the results shown in Figure 1 and 4 is that when the temperature dependent part of the electronic structure (Fermi-Dirac distribution and electronic entropy) is added to the Gibbs energies of the two models, the "DFT" is below that of the full "DFT+SO+OP" theory because the lattice-vibration contribution is greater.

In Figure 5 we show the Gibbs energies obtained from adding the electronic and lattice-vibration contributions at constant volumes (16.2 Å^3 and 15.6 Å^3) together with our CALPHAD Gibbs energy for PuC. The lesser (DFT) theory lies below the full (DFT+SO+OP) theory and appears to be in better agreement with the CALPHAD result.

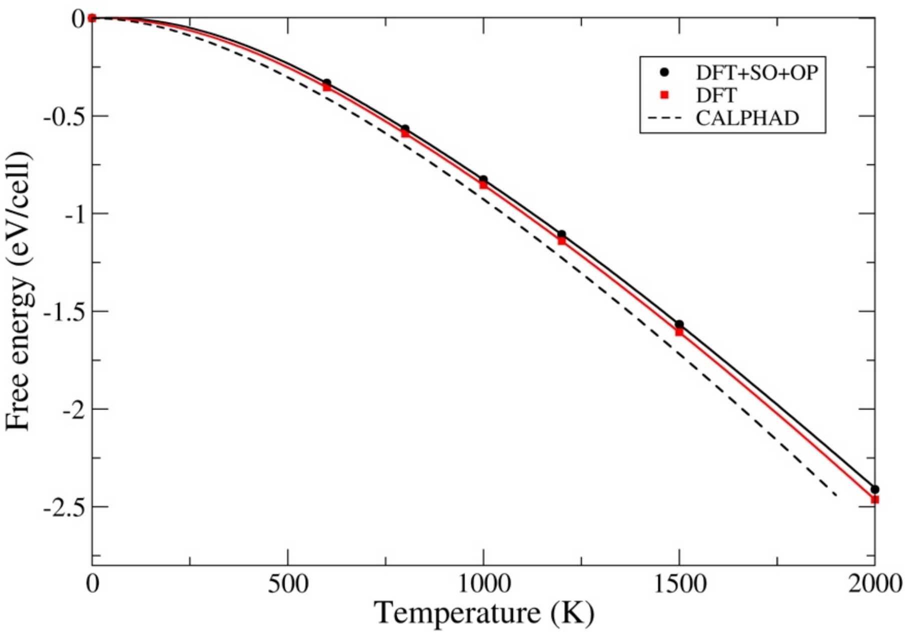

Figure 5. Free energies from SCAILD lattice contribution and electronic structure at volumes of 15.6 (DFT) and 16.2 Å^3 (DFT+SO+OP), respectively. Dashed line shows the CALPHAD Gibbs energy.

This is accidental because important contributions to the Gibbs energy are still missing in the first-principles modeling. First, removing the constraint of a fixed atomic volume, i.e., by accounting for thermal expansion, lowers the Gibbs energies a substantial amount. It comes with a significant computational cost to calculate this contribution, however, because SCAILD needs to be repeated for at least two more volumes (for each temperature) so that the equilibrium volume can be determined. In addition, since we are studying magnetically disordered PuC (over 100 K [45]), there is a simple magnetic contribution due to magnetic disorder [50,51] that we can include:

$$F_{mag}(V,T) = -k_B T ln(2\mu + 1) \quad (4)$$

In this equation, k_B is the Boltzmann constant and μ the total (spin and orbital) magnetic moment. Because orbital polarization, that enhances the magnitude of the orbital moment [5], is addressed in the model the total magnetic moment is small (~ 0.1 μ_B). As mentioned, this is due to a near complete compensation between the spin and orbital contributions. Lastly, there is an electron-phonon-coupling term that we are not considering in the free energy. Accounting for all energy excitations from electrons and phonons and their distributions in a universal fashion is difficult and to our knowledge there is no efficient procedure to accurately determine this contribution.

When we add the missing terms (except the electron-phonon term) to the Gibbs energy, the scalar-relativistic (DFT) energy is significantly below CALPHAD and in our opinion erroneous (not shown). The full theoretical treatment (DFT+SO+OP), on the other hand, produces energies that are above but near that obtained from CALPHAD. In Figure 6 we show our best theory of the Gibbs energy together with CALPHAD for PuC. They are quite close, with the first-principles result slightly above CALPHAD, consistent with the fact that electron-phonon interaction is neglected in the ab initio model.

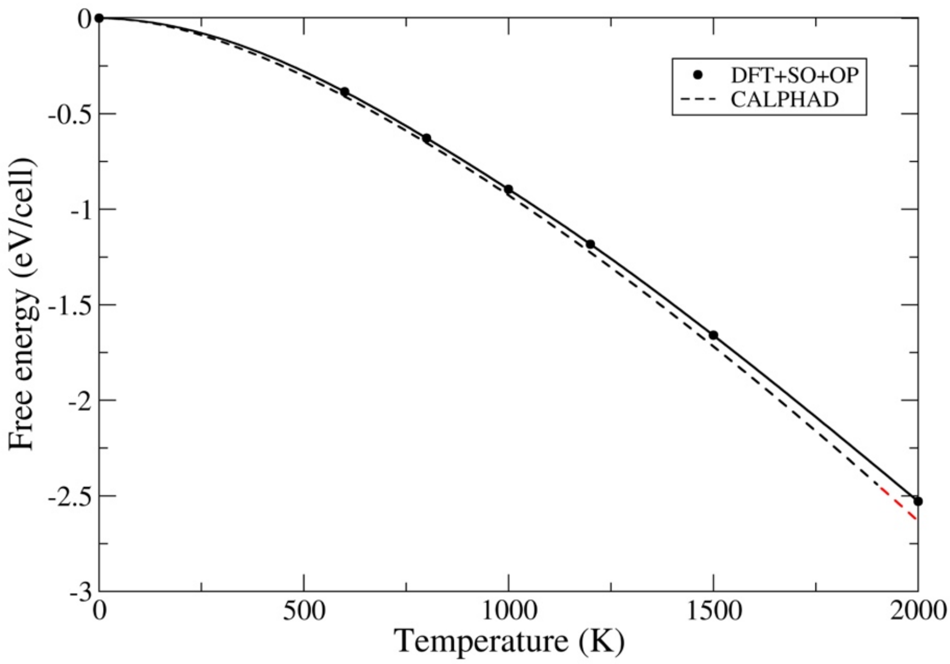

Figure 6. Free energies from our best first-principles calculation and CALPHAD. Above about 1800 K the CALPHAD energy is extrapolated as shown by the red color of the dashed line.

In order to make direct contact with experimental data we also calculate the specific heat at constant pressure, C_p. We compare anharmonic theory (SCAILD and DFT+SO+OP) with lower-level quasi-harmonic theory within the Debye-Grüneisen model. This comparison allows us to evaluate the importance of anharmonicity at higher temperatures. In addition, we calculate CALPHAD C_p for ideal PuC and $PuC_{0.869}$ for a better understanding of the possible significance of sub-stoichiometry. Three sets of experimental data [52-54] are collected for comparison with theory. These data sets are shown in Figure 7 where we also plot the free-electron contribution to C_p obtained from this simple Sommerfeld assumption [55]:

$$C_p^{el}(T) = \frac{\pi^2}{3} D(E_F) k_B^2 T \quad (5)$$

Here, $D(E_F)$ is the electronic density of states at the Fermi level that is extracted from the first-principles electronic structure (DFT+SO+OP).

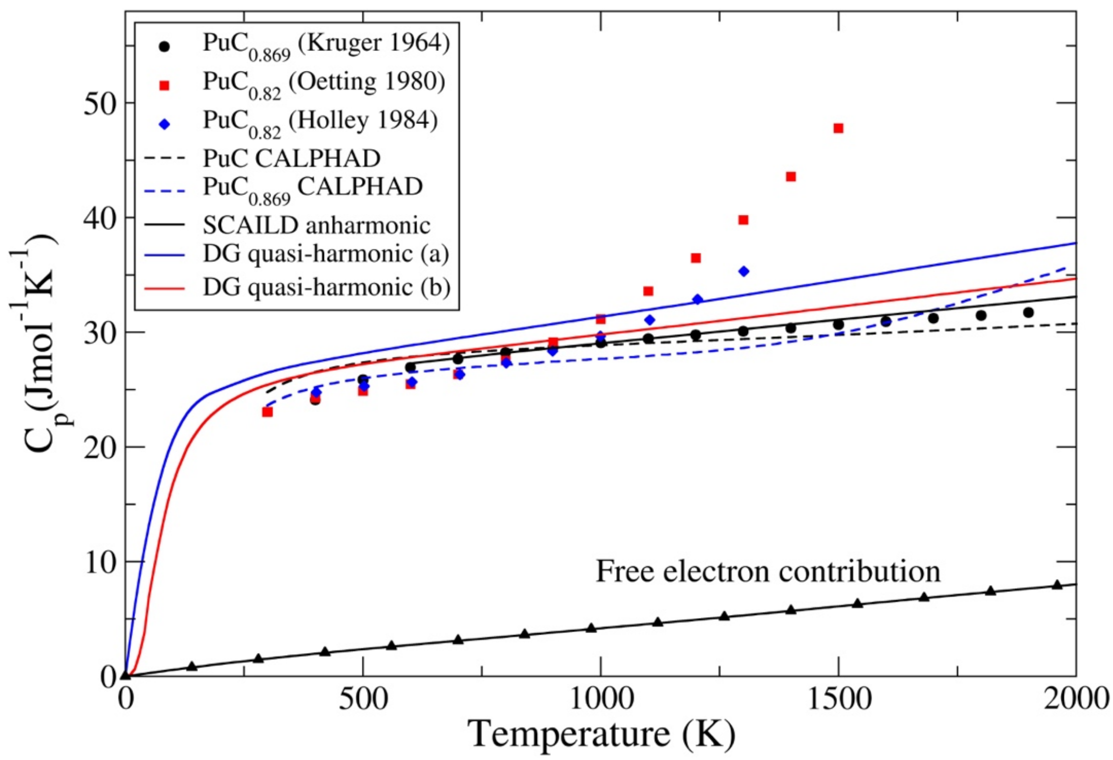

Figure 7. Measured and calculated specific heats at constant pressure, C_P. The solid square (red), diamond (blue), and circle (black) are experimental data sets from Refs. [52-54]. Dashed lines refer to results from CALPHAD. The solid black, blue, and red lines without symbols refer to our best anharmonic theory and two parameterizations of quasi-harmonic Debye-Grüneisen theory. The solid black line with triangles shows the calculated free-electron contribution to C_P.

Perhaps the most glaring aspect of Figure 7 is that the three experimental data sets deviate strongly above 1000 K. To a degree, the difference may be explained by different stoichiometry of the samples, but two of samples have the same stoichiometry. Contradictory experimental data complicates the CALPHAD assessments and the corresponding results become more uncertain. The CALPHAD data show, consistent with experiments, that the stoichiometry does influence C_P to an extent. Our anharmonic theory agrees fairly well with all experimental and CALPHAD data up to 1000 K, but only with the Kruger and Savage [52] and the PuC-specific CALPHAD results above 1000 K. Not surprisingly, it agrees somewhat less favorably with CALPHAD for $PuC_{0.869}$. Furthermore, Figure 7 suggests that the quasi-harmonic treatments, both the (a) and (b) variants (see Computational Methods section 2.2), deviate from CALPHAD and anharmonic theory for PuC above 1000 K. This is consistent with our findings for UN where the quasi-harmonic approach was shown to be increasingly inaccurate at temperatures above 1000 K [14].

4. Summary and discussion

We calculate thermodynamical properties; lattice dynamics, free energies, and heat capacities for ideal-stoichiometry plutonium monocarbide. The highest level of theory includes spin-orbit coupling and orbital-orbital coupling (orbital polarization) for the DFT-GGA electronic structure. This approach assumes delocalized (band) 5f electrons on plutonium and a direct comparison with the experimental photoelectron spectroscopy confirms that this is appropriate for PuC. This interpretation of the 5f electrons is consistent with the calculated Pu-C and Pu-Pu distances (2.52 and 3.57 Å, respectively). Namely, the Pu-Pu distance is close to the Hill limit (~ 3.4 Å) [56] that is an approximate criteria for 5f-band formation.

The thermal properties are obtained from combining our advanced DFT to a temperature-dependent self-consistent phonon scheme that includes strong anharmonic lattice dynamics. We show that this level of electronic-structure theory and lattice dynamics are necessary to reproduce the CALPHAD Gibbs energy and produce consistent specific-heat data. The consistency between our first-principles modeling, CALPHAD, and experiment is further explored by comparing PuC formation enthalpies. The formation enthalpy for PuC is calculated as the DFT+SO+OP total energy difference between the compound and its solid-form constituents, i.e., carbon (α-C, graphite) and α-plutonium; E(PuC) – E(α-Pu) – E(α-C) = -21 kJ/mol. Here, all phases are carefully relaxed (not a trivial task for α-plutonium [5]). The first-principles formation enthalpy is in reasonable agreement with results from CALPHAD (-26.4 kJ/mol) and the experimental values, that range from -15.4 to -25.3 kJ/mol [42,54]. Hence, there is favorable coherence in the thermodynamical properties between modeling and experiments.

The correlation between theoretical and experimental specific heats is obscured by the fact that plutonium monocarbide forms with a deficiency of carbon atoms, i.e., PuC_{1-x}, where x is ~ 0.1. One can capture this carbon deficiency in supercell calculations by removing carbon atoms and creating vacancies on the carbon sites. Specifically, by removing one carbon atom from a 16-atom supercell, we can study the Pu_8C_7 compound, i.e., PuC_{1-x}, where x = 0.125. The calculation is performed with VASP and the full SO+OP treatment, allowing for structural relaxation of the supercell with the vacancy. It turns out that the relaxation effects are small but the atomic volume increases significantly with a corresponding softening of the bulk modulus. Complementary to these supercell calculations, we conduct an EMTO-CPA investigation of a disordered PuC_{1-x} system where C/Pu = 0.90, and 10% of the carbon atoms are replaced by vacancies but without structural relaxation. In other words, the carbon atoms and vacancies are randomly distributed on the carbon-type sub-lattice with 10% probability of being a vacancy and 90% probability of being a carbon atom. Consistent with the supercell results, our disorder EMTO-CPA model finds an increase in atomic volume and a decrease of the bulk modulus when carbon is eliminated. This behavior is also in agreement with a recent theoretical study [57] of the stoichiometry in PuC. From the computed bonding energetics of the carbon-deficient system we apply the quasi-harmonic treatment [33] and compare that with an analogous calculation for the ideal PuC system for VASP and EMTO (not shown). The difference in the specific heats, due to sub-stoichiometry, proves to be small for both methods and it cannot fully explain the sensitivity to the stoichiometry reflected in the experimental heat capacity.

Author Contributions: Conceptualization, P.S.; methodology, P.S., A.L., A.P., E.E.M.; writing-review and editing, P.S., A.L., A.P., E.E.M., C. Wu. All authors have read and agreed to the published version of the manuscript.

Funding:

Acknowledgments: We thank B. Sadigh for helpful discussions. This work was performed under the auspices of the U.S. DOE by LLNL under Contract DE-AC52-07NA27344

Conflicts of Interest: The authors declare no conflict of interest.

References

1. Petit, L.; Svane, A.; Szotek, Z.; Temmerman, W.M.; Stocks, G.M. Electronic structure and ionicity of actinide oxides from first principles. *Phys. Rev. B* **2010**, *81*, 045108(1)-045108(11). https://doi.org/10.1103/PhysRevB.81.045108
2. Wen, X.-D.; Martin, R.L.; Henderson, T.M.; Scuseria, G.E. Density functional theory studies of electronic structure of solid state actinide oxides. *Chem. Rev.* **2013**, *113*, 1063-1096. https://doi.org/10.1021/cr300374y
3. Moore, K.T.; van der Laan, G. Nature of the 5f states in the actinide metals. *Rev. Mod. Phys.* **2009**, *81*, 235-298. https://doi.org/10.1103/RevModPhys.81.235
4. Söderlind, P. First-principles phase stability, bonding, and electronic structure of actinide metals. *J. Electron Spectr. Rel. Phenom.* **2014**, *194*, 2-7. https://doi.org/10.1016/j.elspec.2013.11.009
5. Söderlind, P.; Landa, A.; Sadigh, B. Density-functional theory for plutonium. *Adv. Phys.* **2019**, *68*, 1-47. https://doi.org/10.1080/00018732.2019.1599554
6. Sadigh, B.; Kutepov, A.; Landa, A.; Söderlind, P. Assessing relativistic effects and electron correlation in the actinide metals Th to Pu. *Appl. Sci.* **2019**, *9*, 5020(1)-5020(14). https://doi.org/10.3390/app9235020

7. Amadon, B. First-principles DFT+DMFT calculations of structural properties of actinides: Role of Hund's exchange, spin-orbit coupling, and crystal structure. *Phys. Rev. B* **2016**, *94*, 115148; Erratum in **2018**, *97*, 039903(1)-039903(14). https://doi.org/10.1103/PhysRevB.94.115.148
8. Savrasov, S.Y.; Kotliar, G. Ground-state theory of δ-Pu. *Phys. Rev. Lett.* **2000**, *84*, 3670-3673. https://doi.org/10.1103/PhysRevLett.84.3670.
9. Marianetti, C.A.; Haule, K.; Kotliar, G.; Fluss, M.J. Electronic coherence in δ-Pu: A dynamical mean-field theory study. *Phys. Rev. Lett.* **2008**, *101*, 056403(1)-056403(4). https://doi.org/10.1103/PhysRevLett.101.056403
10. Söderlind, P.; Zhou, F.; Landa, A.; Klepeis, J.E. Phonon and magnetic structure in δ-plutonium from density-functional theory. *Sci. Rep.* **2015**, *5*, 15958(1)-15958(6). https://doi.org/10.1038/srep15958
11. Wen, X.-D.; Martin, R.L.; Scuseria, G.E.; Rundin, S.P.; Batista, E.R. A screened hybrid DFT study of actinide oxides, nitrides, and carbides. *J. Phys. Chem. C* **2013**, *117*, 13122-13128. https://doi.org/10.1021/jp403141t
12. Pogány, P.; Kovács, A.; Visscher, L.; Konings, R.J.M. Theoretical study of actinide monocarbides (ThC, UC, PuC, and AmC). *J. Chem. Phys.* **2016**, *145*, 244310(1)-244310(9). https://doi.org/10.1063/1.4972812
13. Srivastava, D.; Garg, S.P.; Goswami, G.L. Thermodynamic analysis of mixed carbide, carbonitride, and nitride fuels for fast breeder reactors. *J. Nucl. Matter* **1989**, *161*, 44-56. https://doi.org/10.1016/0022-3115(89)90461-3.
14. Söderlind, P.; Landa, A.; Perron, A.; Sadigh, B.; Heo, T.W. Ground-state and thermodynamical properties of uranium mononitride from anharmonic first-principles theory. *Appl. Sci*. **2019**, *9*, 3914(1)-3914(11). https://doi.org/10.3390/app9183914
15. Perdew, J.P.; Burke, K.; Ernzerhof, M. Generalized gradient approximation made simple. *Phys. Rev. Lett.* **1996**, *77*, 3865-3868. https://doi.org/10.1103/PhysRevLett.77.3865
16. Wills, J.M.; Alouani, M., Andersson, P., Delin, A., Eriksson, O., Grechnyev, O. *Full-Potential Electronic Structure Method*; Publisher: Springer-Verlag, 2010.
17. Eriksson, O.; Brooks, M.S.S.; Johansson, B. Orbital polarization in narrow-band systems: Application to volume collapses in light lanthanides. *Phys. Rev. B* **1990**, *41*, 7311-7314. https://doi.org/10.1103/PhysRevB.41.7311
18. Hill, R. The elastic behaviour of a crystalline aggregate. *Proc. Phys. Soc.* **1952**, *A65*, 349-354.
19. Souvatzis, P.; Eriksson, O.; Katsnelson, M.I.; Rudin, S.P. The self-consistent ab initio lattice dynamical method. *Com. Mat. Sci*. **2009**, *44*, 888-894. https://doi.org/10.1016/j.commatsci.2008.06.016.
20. Blöchl, P.E. Projector augmented-wave method. *Phys. Rev. B* **1994**, *50*, 17953-17979. https://doi.org/10.1103/PhysRevB.50.17953
21. Kresse, G.; Furthmüller, J. Efficient iterative schemes for *ab initio* total-energy calculations using a plane-wave basis set. *Phys. Rev. B* **1996**, *54*, 11169-11186. http://doi.org/10.1103/PhysRevB.54.11169
22. Kresse, G.; Joubert, D. From ultrasoft pseudopotentials to the projector augmented-wave method. *Phys. Rev. B* **1999**, *59*, 1758-1775. https://doi.org/10.1103/PhysRevB.59.1758
23. Faulkner, J.S. The modern theory of alloys. *Prog. Mater. Sci.* **1982**, *27*, 1-187. https://doi.org/10.1016/0079-6425(82)90005-6
24. Vitos, L. Total-energy method based on the exact muffin-tin orbital theory. *Phys. Rev. B* **2001**, *64*, 014107(1)-014107(11). https://doi.org/10.1103/PhysRevB.64.014107
25. Vitos, L.; Abrikosov, I.A.; Johansson, B. Anisotropic lattice distortions in random alloys from first-principles theory. *Phys. Rev. Lett.* **2001**, *87*, 156401(1)-156401(4). https://doi.org/10.1103/PhysRevLett.87.156401
26. Söderlind, P.; Grabowski, B.; Yang, L.; Landa, A.; Björkman, T.; Souvatzis, P.; Eriksson, O. High-temperature phonon stabilization of γ-uranium from relativistic first-principles theory. *Phys. Rev. B* **2012**, *85*, 060301(1)-060301(4). https://doi.org/10.1080/00018732.2019.1599554
27. Söderlind, P. Lattice dynamics and elasticity for ε-plutonium. *Sci. Rep.* **2017**, *7*, 1116(10)-1116(6). https://doi.org/10.1038/s41598-017-01034-6
28. Moruzzi, V.L.; Janak, J.F.; Schwarz, K. Calculated thermal properties of solids. *Phys. Rev. B* **1988**, *37*, 790-799. https://doi.org/10.1103/PhysRevB.37.790
29. Slater, J.C. Introduction to chemical physics; Publisher: McGraw-Hill: New York, 1939.
30. Dugdale, J.S.; MacDonald, D.K.C. The thermal expansion of solids. *Phys. Rev.* **1953**, *89*, 832-834. https://doi.org/10.1103/PhysRev.89.832

31. Morse, P.M. Diatomic molecules according to wave mechanics. II. Vibrational levels. *Phys. Rev*. **1929**, *34*, 57-64. https://doi.org/10.1103/PhysRev.34.57
32. Otero-de-la Roza, A.; Luaña. Gibbs2: A new version of the quasi-harmonic model code. I. Robust treatment of the static data. *Comput. Phys. Commun*. **2011**, *182*, 1708-1720. https://doi.org/10.1016/j.cpc.2011.04.016
33. Söderlind, P.; Nordström, L.; Yongming, L.; Johansson, B. Relativistic effects on the thermal expansion of the actinide elements. *Phys. Rev. B* **1990**, *42*, 4544-4552. https://doi.org/10.1103/PhysRevB.42.4544
34. Birch, F. Finite elastic strain of cubic crystals. *Phys. Rev*. **1947**, *71*, 809-824. https://doi.org/10.1103/PhysRev.71.809
35. Kaufman, L.; Bernstein, H. *Computer calculation of phase diagrams with special reference to refractory metals*; Publisher: Academic Press, USA, 1970.
36. Saunders, N.; Miodownik, A. *CALPHAD calculation of phase diagrams: A comprehensive guide*; Publisher: Elsevier Science, 1998.
37. Lukas, H.; Fries, S.; Sundman, B. *Computational thermodynamics: The CALPHAD method*; Publisher: Cambridge University Press, 2007.
38. Bajaj, S.; Landa, A.; Söderlind, P.; Turchi, P.E.A.; Arroyave, R. The U-Ti system: Strengths and weaknesses of the CALPHAD method. *J. Nucl. Mater*. **2011**, *419*, 177–185. https://doi.org/10.1016/j.jnucmat.2011.08.050
39. Perron, A.; Turchi, P.E.A.; Landa, A.; Söderlind, P.; Ravat, B.; Oudot, B.; Delaunay, F.; Kurata, M. Thermodynamic re-assessment of the Pu-U system and its application to the ternary Pu-U-Ga system. *J. Nucl. Mater*. **2014**, *454*, 81-95. https://doi.org/10.1016/j.jnucmat.2014.07.051
40. Perron, A.; Turchi, P.E.A.; Landa, A.; Söderlind, P.; Ravat, B.; Oudot, B.; Delaunay. The Pu-U-Am system: an ab initio informed CALPHAD thermodynamic study. *J. Nucl. Mater*. **2015**, *458*, 425-441. https://doi.org/10.1016/j.jnucmat.2014.12.101
41. Moore, E.E.; Turchi, P.E.A.; Landa, A.; Söderlind, P.; Oudot, B.; Belof, J.L.; Stout, S.A.; Perron, A. Development of a CALPHAD thermodynamic database for Pu-U-Fe-Ga alloys. *Appl. Sci*. **2019**, *9*, 5040(1)-5040(25). https://doi.org/10.3390/app9235040
42. Guéneau, C.; Dupin, S.; Sundman, B.; Martial, C.; Dumas, J.-C.; Gossé, S.; Chatain, S.; De Bruycker, F.; Manara, D.; Konings, R.J.M. Thermodynamic modelling of advanced oxide and carbide nuclear fuels: Description of the U-Pu-O-C systems. *J. Nucl. Mater*. **2011**, *419*, 145-167. https://doi.org/j.jnucmat.2011.07.033
43. Gouder, T.; Havela, L.; Shick, A.B.; Huber, F.; Wastin, F.; Rebizant, J. Variability of 5f states in plutonium carbides. *J. Phys.: Condens. Matter* **2007**, *19*, 476201(1)-476201(11). https://doi.org/10.1088/0953-8984/19/47/476201
44. Söderlind, P.; Landa, A.; Sadigh, B. Density-functional investigation of magnetism in δ-Pu. *Phys. Rev. B* **2002**, *66*, 205109(1)-205109(6). https://doi.org/10.1103/PhysRevB.66.205109
45. Green, J.L.; Arnold, G.P.; Leary, J.A.; Nereson, N.G. Chrystallographic and magnetic ordering studies of plutonium carbides using neutron diffraction. *J. Nucl. Mater.* **1970**, *34*, 281-289. https://doi.org/10.1016/0022-3115(70)90194-7
46. Yang, R.; Tang, B.; Gao, T.; Ao, B. Structural, magnetic, electronic and optical properties of PuC and $PuC_{0.75}$: A hybrid density functional study. *J. Nucl. Mater.* **2016**, *473*, 54-60. https://doi.org/j.jnucmat.2016.02.025
47. Verma, A.K.; Kaushik, S.; Singh, D.; Yadav, R.R. Elastic and thermal properties of carbides of U, Pu, and Am. *J. Phys. Chem. Sol.* **2019**, *133*, 21-27. https://doi.org/10.1016/j.jpcs.2019.05.006
48. Söderlind, P.; Landa, A.; Klepeis, J.E.; Suzuki, Y.; Migliori, A. Elastic properties of Pu metal and Pu-Ga alloys. *Phys. Rev. B* **2010**, *81*, 224110(1)-224110(9). https://doi.org/10.1103/PhysRevB.81.224110
49. Krajewski, A.; D'Alessio, L.; De Maria, G. Physio-chemical and thermophysical properties of cubic binary alloys. *Cryst. Res. Technol.* **1998**, *33*, 341-374. https://doi.org/10.1002/(SICI)1521-4079(1998)33:3<341::AID-CRAT341>3.0.CO;2-I
50. Grimvall, G. Spin disorder in paramagnetic fcc iron. *Phys. Rev. B* **1989**, *39*, 12300-123001. https://doi.org/10.1103/PhysRevB.39.12300
51. Wang, Y. Classical mean-field approach for thermodynamics: Ab initio thermophysical properties of cerium. *Phys. Rev. B* **2000**, *61*, R11863-R11866. https://doi.org/10.1103/PhysRevB.61.R11863
52. Kruger, O.L.; Savage, H. Heat capacity of plutonium monocarbide from 400° to 1300° K. *J. Chem. Phys.* **1964**, *40*, 3324-3328. https://doi.org/10.1063/1.1725001

53. Oetting, F.L. The chemical thermodynamics of nuclear materials: IV. The high temperature enthalpies of plutonium monocarbide and plutonium sesquicarbide. *J. Nucl. Mater*. **1980**, *88*, 265-272. https://doi.org/10.1016/0022-3115(80)90282-2
54. Holley, C.E.; Rand, M.H.; Storms, E.K. *The chemical thermodynamics of actinide elements and compounds. Part 6: the actinide carbides*; Publisher: IAEA, Vienna, 1984, pp. 53-72.
55. Grimvall, G. *Thermophysical properties of materials*; Publisher: Elsevier, New York, 1986, pp. 157-172.
56. Hill, H.H. in *Plutonium 1970 and other actinides*, Ed. Miner, W.D.; Publisher: The metallurgical society of the AIME, New York, 1970, pp. 2-19.
57. Lai, C.; Hu, Y.; Qiu, R. Thermodynamical stability of substoichiometric plutonium monocarbide from first-principles calculations. *Phys. Chem. Chem. Phys*. **2020**, *22*, 9009-9013. https://doi.org/10.1039/c9cp06807d